Marine and Petroleum Geology 157 (2023) 106467

Contents lists available at ScienceDirect

Marine and Petroleum Geology

journal homepage: www.elsevier.com/locate/marpetgeo

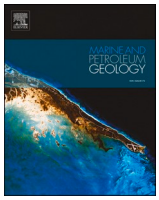

In situ bottom sediment temperatures in the Siberian arctic seas: Current state of subsea permafrost in the kara sea vs laptev and east Siberian seas

B. Bukhanov [a,*], E. Chuvilin [a], M. Zhmaev [a,b], N. Shakhova [b,c,d], E. Spivak [c,d], O. Dudarev [c,d], A. Osadchiev [e,f,d], M. Spasennykh [a], I. Semiletov [c,d]

[a] Skolkovo Institute of Science and Technology, Skolkovo Innovation Centre, Moscow, Russia
[b] Sadovsky Institute of Geosphere Dynamics, Moscow, Russia
[c] V.I. Il'ichev Pacific Oceanographic Institute (POI), Far East Division of the Russian Academy of Science, Vladivostok, Russia
[d] Tomsk State University, Tomsk, Russia
[e] Shirshov Institute of Oceanography, Russian Academy of Sciences, Moscow, Russia
[f] Moscow Institute of Physics and Technology, Dolgoprudny, Russia

ARTICLE INFO

Keywords:
Arctic shelf
Bottom sediments
Sediment temperature
Freezing point
Subsea permafrost
Continental slope
Kara sea
Plumes of great siberian rivers

ABSTRACT

Features of sediment temperature on the shelf and continental slope areas of the Russian Arctic seas and its physical properties are important for understanding the current state of subsea permafrost and the gas hydrates stability zone. New data are reported for the Kara Sea region where the bottom sediment temperatures are influenced by warming effects from great Siberian rivers and the Atlantic currents. The data collected during marine expeditions in 2019–2022 are combined with results of earlier marine studies, drilling operations, and geophysical surveys in the Laptev and East Siberian seas, in order to identify major trends of *in situ* temperature and properties distribution of bottom sediments in the Russian Arctic region.

Most (85%) of bottom sediments in the Kara Sea shelf, as well as in the Laptev and East Siberian shelves, consist of water-saturated silty clay and silt with rather uniform particle size distribution. The obtained thermal conductivity and heat capacity values for the Kara Sea sediments agree with the values of 1.0 W/(m·K) and 2900 kJ/m^3, respectively, obtained previously from other Arctic seas. Thermal conductivity becomes up to 40% higher depthward from 0 to 2 m subbottom depth, possibly, because of lower moisture content and porosity in more lithified sediments.

The bottom sediment temperatures in the Arctic seas are distributed unevenly, especially in the Kara Sea shelf (from +5.0 °C in the west to −1.4 °C in the east), where the high sediment temperatures in the western and central parts of the Kara Sea being due to the effect of warm water inputs. The distribution of bottom sediment temperatures correlates well with distribution of relic subsea permafrost. Ice-bearing permafrost in the Siberian Arctic shelf extends from the shoreline till sea depths of 80–100 m, within the respective offshore distances of ~800–1000 km in some areas, but permafrost remnants may exist locally at sea depths within 120 m. Buried 100–600 m thick continuous subsea permafrost may occur in the Kara, Laptev, and East Siberian shelves under unfrozen (cryotic) saline shallow sediments. However, subsea permafrost is discontinuous and sporadic at sea depths ~70 m and more. Thus, the bottom sediment temperature features in the Arctic seas can be used as a proxy of subsea permafrost extent contenting intrapermafrost and subpermafrost gas and gas hydrate accumulations.

1. Introduction

The Russian Arctic shelf is a rapidly developing region with good economic prospects due to rich oil and gas resources (Kontorovich et al., 2010; Gulas et al., 2017; Dziublo and Storozheva, 2021; Egorov et al., 2021) and transportation possibilities via the transshipment hub along the Northern Sea Route (Hermann et al., 2022; Makarov et al., 2022). Meanwhile, although being of great social and economic value, the Arctic shelf territory, especially its eastern part, remains poorly and unevenly investigated. Setting up comprehensive studies is problematic

* Corresponding author.
E-mail address: B.Bukhanov@skoltech.ru (B. Bukhanov).

https://doi.org/10.1016/j.marpetgeo.2023.106467
Received 16 May 2023; Received in revised form 9 August 2023; Accepted 16 August 2023
Available online 19 August 2023

because of vast ice spaces, harsh weather conditions, short shipping seasons, and thus time-consuming and logistically challenging field observations. More problems are caused by the presence of subsea permafrost, which is hard to study because drilling and other surveys are risky and expensive (Kozlov, 2006; Shakhova et al., 2010a; Loktev et al., 2012, 2017; Sergienko et al., 2012; Winkler, 2018). The thickness of ice-rich subsea permafrost and the depth to its table have been constrained by a modest amount of drilling and geophysical surveys in the nearshore zone (Shakhova et al., 2014, 2017; Overduin et al., 2015, 2016; Koshurnikov et al., 2016) and numerical simulation. However, numerical models m ostly stem from unreliable input parameters (paleoclimatic scenarios, seafloor temperature variations, heat flux density, thermal parameters of sediments, etc.), depend on the resolution and quality of reference geological models, and thus provide only approximate results. The data on the thermal state, composition and properties of bottom sediments in the Russian Arctic shelf, especially its eastern sector, are limited to few publications (Grigoriev, 1966; Fartyshev, 1993; Grigoriev et al., 1996; Cheverev et al., 2007; Shakhova and Semiletov, 2007; Chuvilin et al., 2013, 2021; Günther et al., 2013), as well as the estimates of *in situ* bottom sediment temperatures (Shakhova and Semiletov, 2007; Loktev et al., 2012; Chuvilin et al., 2021a; Shakhova et al., 2017). On the other hand, the temperatures of near-bottom water have been recorded in various databases (e.g., NOAA World Ocean Database) and maps (Vasiliev et al., 2013; Bogoyavlensky et al., 2018, 2021; Shirokov and Vasiliev, 2019). One of the complete hydrological databases, including bottom water temperatures, has been created at the Laboratory for Arctic Research of the V.I. Il'ichev Pacific Oceanographic Institute (POI FEBRAS) as a result of about fifty oceanographic cruises over the East Siberian Arctic seas (1999–2020). Some of the results obtained in those studies were published previously (Luchin et al., 2002; Luchin and Semiletov, 2005; Semiletov et al., 2005, 2016; Shakhova et al., 2014). The bottom water temperature data are often used to infer the *in situ* bottom sediment temperature in the absence of measured evidence (Bogoyavlensky et al., 2018; Matveeva et al., 2020), but this extrapolation is poorly applicable to the Arctic seas. The reason is that the temperature of near-bottom water is more sensitive to such effects as seasonal air temperature variations, sea depth, offshore distance, inflow of riverine water, sea currents, etc. than the more stable temperature of sediments. The bottom sediment temperatures have important implications for the state of subsea permafrost in the Arctic shelf.

Currently the greatest portion of drilling evidence for the existence of subsea permafrost comes from the Kara Sea which, along with numerical models, made basis for several maps of ice-bearing and unfrozen cryotic ($t < 0$ °C) sediments (Melnikov and Spesivtsev, 1995; Rokos et al., 2009; Rekant and Vasiliev, 2011; Vasiliev et al., 2011). The most detailed information was reported by Gavrilov et al. (2020a) who distinguished continuous, discontinuous, and sporadic relic permafrost offshore. The permafrost thickness varies from 0 to 100 m in the southwestern, northeastern, central, and estuary zones to 100–200 m in the northwestern part (east of 75°E) of the Kara Sea. Discontinuous permafrost in the West Yamal shelf may reach sea depths of 115 m (Portnov et al., 2013; Serov et al., 2015, 2017) while continuous permafrost is restricted to the shoreline within 20 m deep water. However, these estimates are based on a limited data sets and require updating.

Although the field data on the presence of permafrost and cryotic sediments in the East Siberian Arctic Shelf (ESAS), including the Laptev Sea and the East Siberian Sea, are far insufficient, the distribution of subsea permafrost in the Laptev and East Siberian seas have been simulated in several models based on theoretical ideas of the Arctic permafrost evolution and on analogy with other Arctic territories (Romanovskii et al., 1999, 2003). The simulation results for the state of subsea permafrost were fitted to drilling data from the Dmitry Laptev Strait (Nicolsky and Shakhova, 2010). Later Nicolsky et al. (2012) provided an overview of geothermal studies in the ESAS performed over the 20th century which was used to compile a map of submarine permafrost with reference to the 1-D Transient Heat Flux (SuPerMAP) model (Overduin et al., 2019), taking into account the effect of salt diffusion on degradation of permafrost (Angelopoulos et al., 2019, 2020). Note, that the SuPerMAP model doesn't give the depth of the subsea permafrost table which is a critically important parameter for basic understanding and numerous applications. It has been accepted that reliable modeling of the current permafrost state requires true values of input parameters (seafloor temperature, thermal parameters and freezing point of sediments) specific to certain areas of the Arctic shelf. In general, subsea permafrost at the East Siberian Arctic seas (ESAS) shelf was considered to extend till sea depths of ~80 m and to reach a thickness of 400–500 m (Romanovskii and Tumskoy, 2011; Gavrilov et al., 2020b; Matveeva et al., 2020). Additionally, there is implicit evidence that local zones of relic marine permafrost may exist in the Laptev shelf within 120 m sea depth (Chuvilin et al., 2022). The actual representative data on the state of subsea permafrost are based on drilling and logging data with electromagnetic surveys calibrated against well logs (Koshurnikov et al., 2016; Shakhova et al., 2017). The obtained field data show that the current offshore permafrost is up to 10 °C warmer than that onshore (Shakhova et al., 2014; Yusupov et al., 2022). According to electromagnetic surveys significant part of ESAS permafrost is discontinuous and contains gas and gas hydrate accumulations. In general, marine permafrost extends over large areas in the central and eastern parts of the Kara, East-Siberian, Laptev seas shelf up to 50–100 m isobath, has a thickness of several hundred meters, which degrades at a rate of about 14–18 cm per year (Koshurnikov, 2023).

Warming of the ESAS began >12 thousand years (kyr) ago in the earliest Holocene after the area had been submerged as a result of sea level rise. The temperature of terrestrial permafrost in the Holocene Arctic changed as the mean annual air temperature has become 6–7 °C warmer since the last glacial maximum (Frenzel et al., 1992). Subsea permafrost has been subjected to additional warming induced by sea water which has much warmer mean annual temperatures than air in the ESAS area: −1 °C against −10 °C, respectively. Consequently, the subsea permafrost has grown up to 17 °C warmer for the last 12 kyrs (Romanovskii and Hubberten, 2001). The evolution of subsea permafrost may have multiple controls: the time when it was submerged relative to the time of emergence; thermal state and thickness of permafrost before inundation; coastal morphology and hydro- and lithodynamics; shoreline configuration and retreat rate; pre-existing thermokarst (particular landforms produced by thawing of ice-rich permafrost or melting of ground ice) and thaw lakes; temperature and salinity of bottom water; composition of sediments, including ice content, etc. (Soloviev et al., 1987; Romanovskii et al., 2004, 2005).

Zones of large-scale methane venting discovered in the ESAS (Shakhova et al., 2010a, 2010b, 2014, 2019), as well as those reported from the Barents and Kara seas (Serov et al., 2015, 2017; Andreassen et al., 2017; Semenov et al., 2020), are of special interest in the context of possible climatic consequences of permafrost degradation in the shelf areas. Note that the methane seeps in the Kara Sea found earlier (Serov et al., 2015, 2017) were found inactive in 2021–2022 (*our unpublished data*). Monitoring of the largest vents of bubbling methane (mega-seeps) during years-long projects of comprehensive studies revealed a prominent expansion trend and the ensuing greater emission of methane, a major greenhouse gas, into the atmosphere (Shakhova et al., 2015; Chernykh et al., 2020). The massive methane release from the ESAS discovered in the early 2000s (Shakhova et al., 2010a, 2010b) contradicts the idea of stable subsea permafrost (Romanovskii et al., 2005; Pachauri and Meyer, 2014). Until recently, the thermal state and stability of the ESAS subsea permafrost–hydrate system were estimated mainly by means of modeling, which allowed for two basic degradation mechanisms of subsea permafrost. Fist mechanism is associated with warming effect from permafrost bottom to above by heat coming from deep fault zones (Soloviev et al., 1987; Romanovskii et al., 2005; Shakhova and Semiletov, 2009; Baranov et al., 2019; Bogoyavlensky et al., 2022). The other mechanism from permafrost table degradation is result

of seawater transgression, loss of sea ice and increasing inputs of warm river flow waters (Semiletov et al., 2005, 2016; Shakhova and Semiletov, 2007; Shakhova et al., 2014, 2019). So, the methane emission is controlled by the current thermal state of the subsea permafrost along with environmental factors that affect the stability of both permafrost and gas hydrates (Shakhova and Semiletov, 2009; Shakhova and Semiletov, 2009; Lobkovskiy, 2020). This inference is consistent with the results of physical modeling showing high sensitivity of gas hydrates in shallow subsea permafrost to external effects (especially, temperature changes). Therefore, they can dissociate already at temperatures 1–2 °C below the freezing point of pore ice (Chuvilin et al., 2019), while the frozen and intrapermafrost hydrate-bearing sediments become more permeable and can no longer seal the methane released by the hydrate dissociation, despite the presence of pore ice (Chuvilin et al., 2021b). This fact undermines the idea of a solid permafrost lid over the subsea gas reservoirs. With the amount of CH_4 preserved in the ESAS shallow sediments and the thawing rates of subsea permafrost (Shakhova et al., 2017), CH_4 emission can increase in several times.

Today there is another point of view about the current state of subsea permafrost in the Arctic seas, which is based on the analysis and interpretation of marine seismic data by JSC MAGE (Marine Arctic Geological Expedition, Russia) obtained in the period 2007–2016 (Bogoyavlensky et al., 2023). According to the presented results, the distribution of subsea permafrost on the shelf of the Laptev and East Siberian seas is significantly less than other scientists suggest, due to its more significant degradation (approx. 60%). Thus, the presence of subsea permafrost approximately corresponds to the 60 m isobath and characterizes ~81% of the Laptev Sea shelf territory, and ~38% of the East Siberian Sea shelf (only its western part). The results of Bogoyavlensky et al. (2023) do not exclude the presence of local sporadic relict permafrost up to 100–120 m isobaths in the Laptev and East Siberian seas. Additionally, it was hypothesized that, as a result of significant degradation of subsea permafrost (about 60% has been already degraded) and its high negative temperature, it should not be expected a large amount of residual permafrost hydrates, and even more so, their significant contribution to the global climate during further degradation of the Arctic shelf permafrost. But in this case, the potential thickness of frozen sediments and the depth of ice-bearing subsea permafrost table are not considered as well as evolution of the hydrate stability zone.

It is currently assumed that the methane emitted by the Arctic seas of Russia is a mix of biogenic and thermogenic origin (Sapart et al., 2017), but more recent evidence from methane seeps in the Laptev shelf suggests prevalence of the deep gas source (Steinbach et al., 2021). Additional data from the northern Laptev Sea shelf confirm that the methane seeps are located within zones of warmer bottom sediment temperatures possibly associated with high heat flux from deformed crust along basement faults (Chuvilin et al., 2022). Unlike the Laptev Sea area, the zones of methane seepage in the East Siberian Sea are free from temperature sediment anomalies, though the gas emitted from the two areas is compositionally similar ($\delta^{13}C$ from −59.6 to −56.7‰ VPDB) may be of the same origin (Chuvilin et al., 2022). The absence of warmer sediments in the methane venting zones of the East Siberian Sea shelf can be explained by a greater thickness of subsea permafrost (according to Romanovskii and Tumskoy (2011)) and younger ages of the seeps. The activity of the East Siberian Sea younger seeps may have been too short to melt out permeable gas chimneys of sufficient sizes and numbers, whereas the older seeps in the Laptev Sea have already produced large permeable zones. This vision is additionally confirmed by the fairly rich methane-oxidizing benthic fauna (*Pogonophore*) on the Laptev Sea shelf seep areas (analogically to methane seep areas in the Kara Sea presented by Malakhov et al., 2023), and the almost complete absence of methanotrophic organisms in the East Siberian younger seeps (*our unpublished data*).

In this respect, further studies with focus on the lateral patterns of sediment temperatures and properties in the shelf and continental slope areas of the Russian Arctic seas are essential for understanding the current state of subsea permafrost and the stability of gas hydrates. These studies are especially important for the Kara Sea which is exposed to the warming effect of both great Siberian rivers (Ob and Yenisei) and the Atlantic waters flowing through the Kara Gate strait from the Barents Sea to the southwestern Kara Sea (southern current). Note that the northern Barents Sea current into the Kara Sea from the area north of the Northern cape of Severnaya Zemlya carries low-temperature water (<0 °C), which may prevent the subsea permafrost from degradation in the central Kara shelf. On the other hand, the warm Fram branch of the Atlantic current affects considerably the temperature patterns of bottom sediments in the St. Anna Trench and along the Eurasia and North America continental slopes. The new data show that the three currents influence the extent and thickness of permafrost in the Kara shelf and complicate the understanding of its evolution and state. The obtained data on bottom sediment temperatures in the Kara Sea indicate on earlier uncounted warming effect from three Atlantic currents reported before (Lien and Trofimov, 2013; Dmitrenko et al., 2014; Osadchiev et al., 2022).

2. Study area and methods

The reported study was part of marine surveys in the Kara Sea during the 86th and 90th cruises of the R/V *Akademik Mstislav Keldysh* (Russia) (Fig. 1a), with a focus on sediments at sea depths from 18 m to 640 m. Additionally, sampling and measurements were performed in the zones of the Kara Sea where seabed methane seeps and methane emission were observed during previous during drilling operations (Loktev et al., 2012, 2017; Portnov et al., 2013) and at the junction of the Fram Strait and Barents Sea branches of Atlantic waters in the St. Anna Trench (Osadchiev et al., 2022) (Fig. 1b). Bottom sediments were sampled at 52 sites, with a box corer, a multicorer, and a gravity corer. Note that the data collected during the AMK-86 cruise of 2021 did not confirm the presence of the seepage area in the Baidaratskaya Bay of the Kara Sea (site 7211 in Fig. 1) reported by Portnov et al. (2013).

During the AMK-86 and AMK-90 cruises, the temperatures of the recovered sediments were measured at ~0.3 m below the seafloor for box corer and multicorer, and at every 10 cm up to 2.9 m for gravity corer. The sediment temperature was measured by needle probes (100 mm in length, 3.5 mm in diameter; sensor precision 0.1 °C). The temperature measurements were taken immediately upon sample recovered on the ship deck. The temperatures measured at 10 cm from the core outer wall were assumed to represent *in situ* bottom sediment temperatures, based on the size of the cores, their thermal inertia, and rapid (5–7 min) recovery onboard (Chuvilin et al., 2021a). At most of the sites, the sea depths of sampling were >20 m, or below the thermocline (~15–18 m), where the water temperature was constant and controlled that of the sediments. Thus, the measured sediment temperatures are presumably constant all the year round.

The thermal parameters of the Arctic shelf sediments were measured using the KD-2 Pro thermal property analyzer immediately after core recovery. KD-2 Pro is equipped with a double needle probe and measures both thermal conductivity (λ, W/(m·K) and heat capacity (C, kJ/(m^3·K). The double probe (model SH-1) consists of two needles, 4.5 cm long and 1.2 mm in diameter, spaced at 1 cm. Each measurement lasts ~2.5 min. The thermal parameters are automatically calculated based on the results of two heating-cooling cycles. The accuracy of KD-2 Pro thermal conductivity and volumetric heat capacity measurements was estimated at 10% and was checked against data for a standard sample supplied with the device. For more details see Chuvilin et al. (2021a).

Some sediment cores were collected for particle size distribution, mineralogy, gravimetric moisture contents (W, %), natural density (ρ, g/cm^3), dry density (ρ_d, g/cm^3), salinity (D_{sal}, %; salt-to-dry sediment weight ratio), and freezing point (T_{bf}, °C). All these data are presented in the Appendix A (Supplementary data). The gravimetric moisture content W is the mass of water (M_w) per mass of dry soil (M_d), in percent:

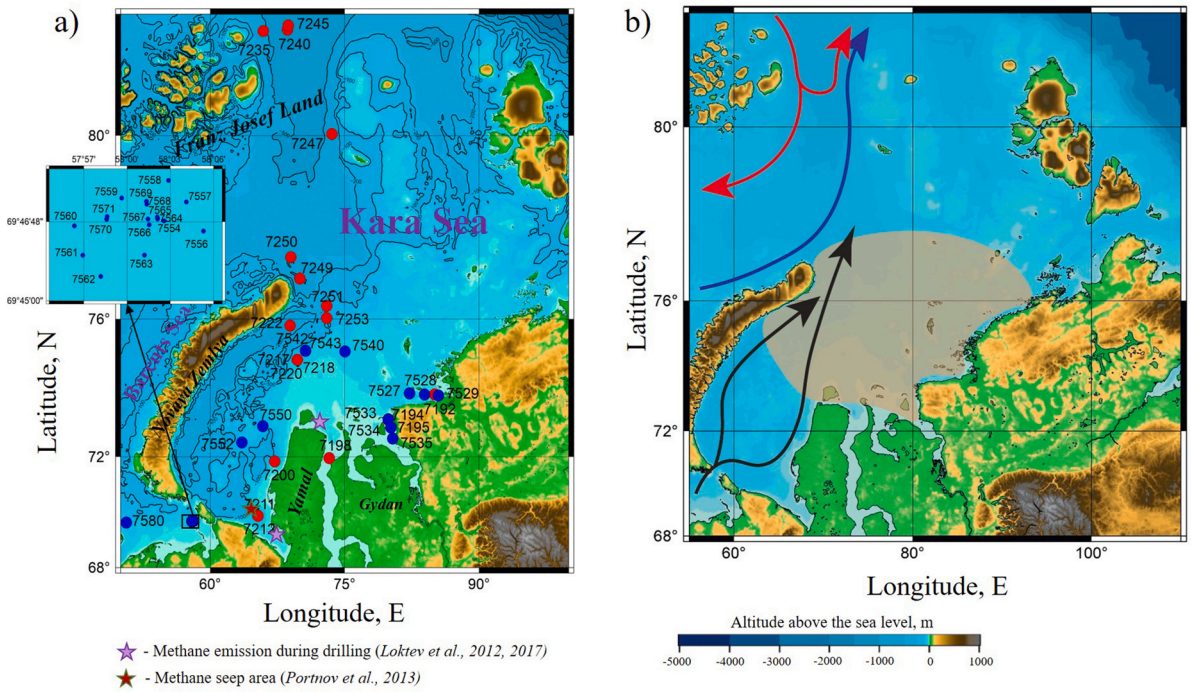

Fig. 1. Location map of study area with sampling sites of cruises AMK-86 (red circles) and AMK-90 (blue circles) (a) and (b) scheme of the main currents in the study area. Numerals are station codes. Black arrows - Barents Sea waters entering through the Kara Gates; Blue arrows - Barents Sea branches of Atlantic water; Red arrows - Fram Strait of Atlantic water; Brown area – Ob' and Yenisey plume.

$$W = \frac{M_w}{M_d} \times 100\% \quad (1)$$

The freezing point of the sediments was determined by the water potential method implying measurements of pore water potential (activity) and subsequent thermodynamic calculations. The results agreed with direct freezing point measurements to ±0.05 °C for different types of soil including Arctic bottom sediments. The particle size distribution of the sampled bottom sediments was analyzed by combined sieving and integral suspension pressure methods (ASTM D422-63, 2007; Durner et al., 2017) by using PARIO from the METER Group. The sediments were documented as recommended in FAO Guidelines for Soil Description (2006).

The data collected during the 86th and 90th cruises of the R/V *Akademik Mstislav Keldysh* were processed jointly with previous data from the 78th and 82nd cruises of 2019 and 2020 on the same R/V (Chuvilin et al., 2021a, 2022), as well as with the data of the SWERUS-C3 2014 Expedition of the I/B *Oden* (Sweden) (Cruise Report SWERUS-C3, 2016 ab) and drilling and geophysical surveys in the Laptev shelf from 2011 through 2014 (Sergienko et al., 2012; Chuvilin et al., 2013; Koshurnikov et al., 2016; Shakhova et al., 2017), in order to reveal general trends in temperature patterns and properties of bottom sediments in the Russian Arctic seas. Additional reference was made to earlier unpublished estimates of *in situ* bottom sediment temperatures from the Laptev and East Siberian shelves obtained by the POI FEBRAS cruises of 2003 and 2005 (Appendix).

3. Results

3.1. In situ bottom sediment temperature

The current state of subsea permafrost in the Kara shelf has been poorly understood as it may include sporadic, discontinuous, or continuous permafrost zones. The available data of marine surveys show strong temperature variations in the bottom sediments depending on geographic location and sea depth (Table 1; Figs. 2 and 3).

Table 1
Average bottom sediment temperatures in the Kara Sea.

Area	Sea depth (m)	Number of stations	Temperature[a] (°C)	Freezing point (°C)
Kara Sea shelf, eastern part	21–33	4	−0.9 ± 0.4[b]	−1.7 ± 0.2
Kara Sea shelf, western part	37–121	5	+2.7 ± 2.1	
Kara Sea shelf, central part	27–130	10	−0.5 ± 0.5	
Continental slope	340–640	6	−0.2 ± 0.2	
Ob and Yenisei estuaries	14–29	6	+0.8 ± 0.8	
Pyasina estuary	14–32	3	+0.1	
Kara Gates Strait	30–45	17	+4.8 ± 0.1	

[a] Average temperatures for upper 0–0.5 m of sediments.
[b] Confidence interval is calculated using standard normal distribution at 0.95 confidence level.

The bottom sediment temperatures were the warmest (+3.0 to +5.0°C) in the southwestern part of the Kara Sea, near the western coast of the Yamal Peninsula, being affected by warm waters that flow from the Barents Sea through the Kara Gates strait and contribute considerably to the near-bottom water temperature pattern in the area. In this respect, relic permafrost in the Yamal western coast is expected to be only sporadic and no thicker than 100 m (Gavrilov et al., 2020a), this being consistent with core data (Rokos et al., 2009). Positive sediment temperatures (0 to +2.0°C) were also obtained for the estuaries of the great Siberian rivers of Ob, Yenisei, and Pyasina, which drain an enormous territory extending far south of the Kara Sea and reach water temperatures of 10–12°C in summer. The inputs of warm river water produce a large 10–15 m thick freshened zone in the central part of the Kara Sea (Osadchiev et al., 2021a, 2021b) and thus cause more warming to near-bottom water in the shallow shelf along the Taimyr Peninsula.

The bottom sediments of the central and eastern Kara Sea have negative temperatures but remain unfrozen and free from pore ice (cryotic) as their freezing point is below the *in situ* temperature. The

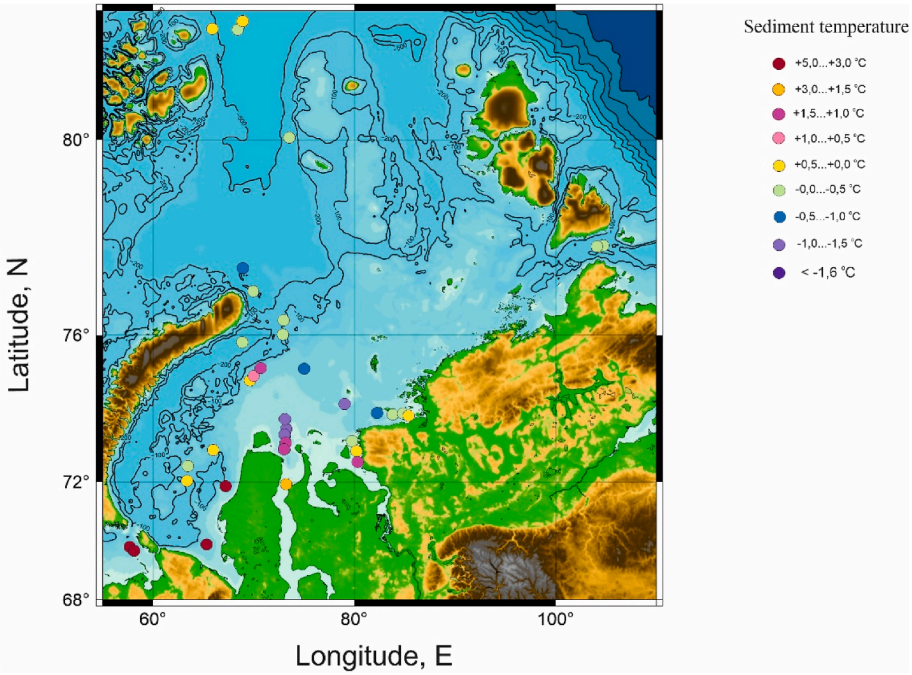

Fig. 2. Temperature patterns of bottom sediments in the Kara Sea.

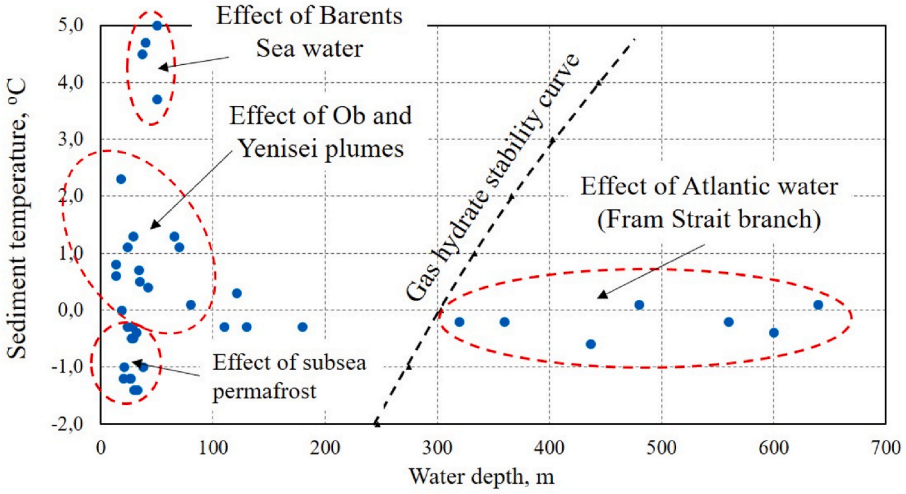

Fig. 3. Sediment temperatures vs. sea depths for the Kara Sea. Gas hydrate stability curve is calculated for pure CH_4 using the thermodynamic equation of Sloan (1998) for seawater (0.6 n NaCl).

temperatures decrease laterally from −0.5°C in the central part to −1.4°C in the eastern part of the Kara Sea, away from the warming effects of the Atlantic waters coming from the Barents Sea and the surface fresh waters carried by the rivers. Correspondingly, the extent of continuous relict subsea permafrost must be restricted to the eastern Kara shelf. The sediments of the northern Kara Sea within the St. Anna Trench (up to 600 m sea depth) exposed to the warming effect of the Fram Strait and Barents Sea branches of Atlantic currents are from −0.4 to +0.1°C (Fig. 3). The methane hydrate stability zone (pure methane and sea water in bulk conditions) for the deepwater Kara Sea (Sloan, 1998), assuming an *in situ* bottom sediment temperature of ~0.0°C, begins at 300 m and deeper on the continental slope (Fig. 3). These estimates based on bottom sediment temperature and water depth data agree generally with the previous results of Bogoyavlensky et al. (2018) and Matveeva et al. (2020), i.e., the hydrate stability zone has a large extent and the depth to its top in the Kara Sea corresponds to the sea depth of deep basins and continental slope. Previously, a similar analysis has already been done by Riedel et al. (2018) for Svalbard Continental Margin. On the base of measured *in situ* sediment temperatures (which was in the range from +3.4 to +4.4°C) methane hydrates stability zone in bottom sediments was predicted at seawater depth 390 m and more. However, despite favorable gas hydrate stability conditions and high gas saturation of bottom sediments (numerous gas vents at a water depth of 400 m) coring did not encounter any gas hydrates (Riedel et al., 2018). Apparently, this situation is associated with a number of uncertainties during assessing the gas hydrate stability zone (the effect of the porous media, actual pore water mineralization and gas composition were not taken into account). So, the gas hydrate stability table may be located at more water depths. It should be noted that within the framework of the current studies on the Kara Sea continental slope from hydrate stability zone (water depth >320 m) no gas hydrates we sampled too, as a result of no methane venting in the investigated sites. In this regard, the

correct assessment of hydrate stability conditions in Arctic marine sediments is still an important problem, which solution is only possible on the basis of analysis *in situ* thermobaric conditions of bottom sediments and soil parameters.

The depth profiles of bottom sediment temperatures obtained from field measurements at several Kara Sea sites show some trends (Fig. 4). The temperature field of the deep-water zone (>200 m) shows low positive gradient, and the temperatures increase only slightly (Fig. 4b), while shelf sediments (<200 m) become cooler with depth, especially in the areas where they are relatively warm (Fig. 4a).

The cooling trend may be implicit proof for the occurrence of buried subsea permafrost, given that some prerequisites of its existence were revealed previously (Melnikov and Spesivtsev, 1995; Rokos et al., 2009). Judging by warm sediment temperatures in the western part of the shelf (station 7251 in Fig. 4a), subsea permafrost there should be sporadic, unlike the −1.0 to +1.0°C shallow sediments in the central (station 7220) and eastern (station 7251) shelf parts, where subsea permafrost may exist deeper beneath the bottom. The trends of depthward cooling at these sites are similar and may have the same cause. Furthermore, bottom sediments have rather low temperatures even at a sea depth of ~130 m, which makes thinking of permafrost extent beyond the currently presumed 80 m limit. Similar temperature anomalies were reported earlier from water depths of ~100–120 m in the Laptev Sea shelf (Chuvilin et al., 2022) and were interpreted as an implicit indicator of relic subsea permafrost.

3.2. Sediments and their physical properties

The sampled bottom sediments from the shelf and deep-water areas of the Kara Sea generally consist of water-saturated silty clay and silt with roughly similar particle size distribution (Fig. 5a; Appendix), which agrees with summarized data from other Arctic seas (Fig. 5b) and well corelates with other geochemical studies (Cruise Report SWERUS-C3, 2016a; Martens et al., 2021; Ulyantsev et al., 2021, 2022; Rusakov and Borisov, 2023). The percentages of clay particles (<0.005 mm) are in the range 20–40% while silt particles (0.062–0.005 mm) reach 50–70%. The sediments have a solid density of ~2.74 g/cm^3, a salinity of ~2.5–3.7%, and contents of total organic carbon (TOC) ~6–7%.

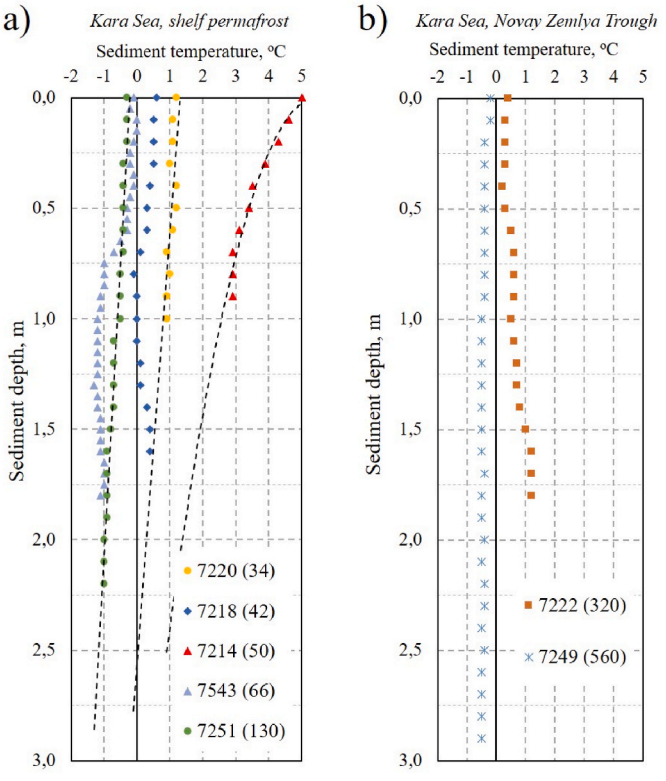

Fig. 4. Depth profile of bottom sediment temperatures in the Kara Sea. Numerals show station code and sea depth in m.

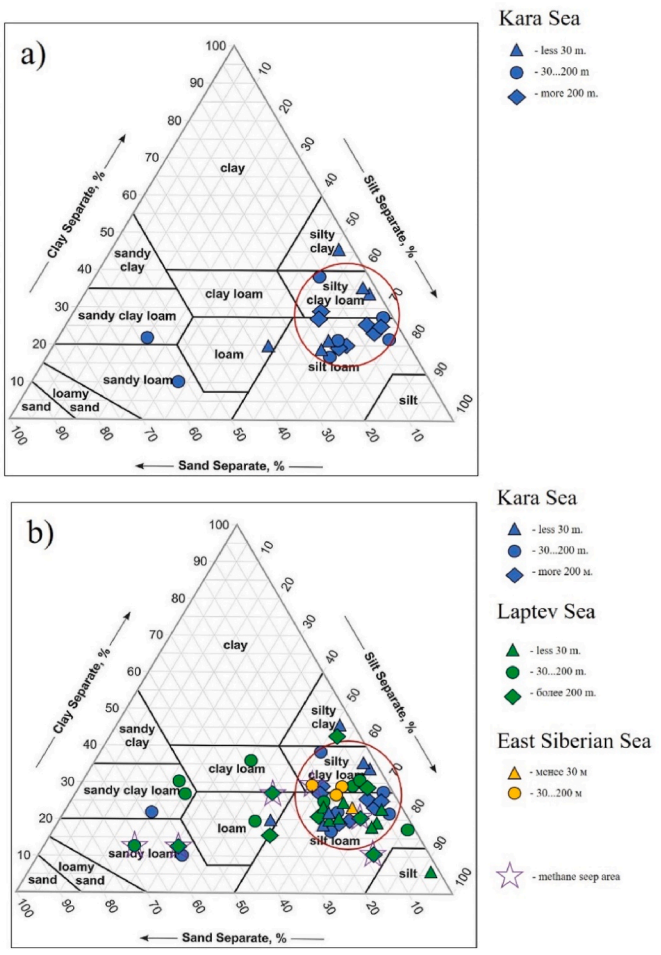

Fig. 5. Particle size distribution of sampled sediments from the Kara Sea (a) and all Arctic Seas (b). Symbols mark different sea depths: <30 m (triangles), 30–200 m (squares), and >200 m (diamonds). Red line encircles 85% of samples.

The values of thermal parameters are almost invariable and average around 1.0 ± 0.1 W/(m·K) for thermal conductivity and 2890 ± 62 kJ/m^3 for bulk heat capacity. These estimates are similar to the respective values for the Laptev and East Siberian seas reported in our previous publications: 1.0 W/(m·K) and 2900 kJ/m^3 (Chuvilin et al., 2013, 2021, 2022). Furthermore, the Kara Sea samples show similar increasing thermal conductivity decreasing heat capacity trends at decreasing water and clay contents while lithification increases (Appendix). Namely, thermal conductivity increases from 0.96 on the surface to 1.35 W/(m·K) at the 2 m subbottom depth while heat capacity decreases from 3000 to 2500 kJ/(m^3·K), with 40% and 17% changes, respectively. Such trends are typical for low lithified bottom sediments (Pribnow et al., 2000; Cruise Report SWERUS-C3, 2016b; Stranne and O'Regan, 2016; Riedel et al., 2018; Zhang et al., 2022) and cause by lower moisture content and porosity in more lithified and deeper sediments.

4. Discussion

The temperatures of bottom sediments in the Kara Sea collected in the course of R/V cruises are unevenly distributed: positive (up to +5.0°C) in the western part and negative (to −1.4 °C) in the east. The warm temperatures in the western Kara Sea result from the effect of

warm Atlantic currents coming from the Barents Sea through the Kara Gates Strait to the southwestern part of the Kara Sea and also from the northwestern part of the Barents Sea and the continental slope to the St. Anna Trench (Fig. 1b). Additional warming effect is due to inputs of relatively warm fresh water from the great Siberian rivers (Ob, Yenisei, and Pyasina) into the central sea part. In this respect, subsea permafrost can be continuous at water depths within 80 m in the central and eastern Kara Sea but is apparently discontinuous to sporadic in the western part.

The patterns of *in situ* sediment temperatures (Fig. 6) generally correlate with the map of ice-bearing marine permafrost in the Kara shelf (see Gavrilov et al. (2020a) for the complete version).

The shelf sediments under water depths of 80–100 m or shallower, where the permafrost is presumably continuous, are as cold as −0.6°C or colder and are located mainly in the central and eastern parts of the Kara Sea. Although having *in situ* temperatures below zero, the seafloor sediments remain unfrozen and free from pore ice (cryotic) because these temperatures are above the freezing point, which provides proofs for the presence of subsea permafrost in the area buried at relatively large subbottom depths. As for the zone of temperatures above −0.6°C, primarily, the western Kara Sea shelf, it correlates with the extent of discontinuous (including sporadic) subsea permafrost. It has warm negative temperatures, no gradient in the thermal field, and is in a pre-thaw state.

In general, the cruise data from the Kara Sea indicate the absence of subsea permafrost at water depths below 100 m, which is consistent with the present views of the Arctic shelf permafrost (Rokos et al., 2009; Rekant and Vasiliev, 2011; Loktev et al., 2012; Matveeva et al., 2020; Overduin et al., 2019). The negative *in situ* sediment temperatures in the Arctic shelf (within 100 m sea depths) can be thus considered as implicit tracers of buried continuous subsea permafrost, while low positive temperatures may be evidence that subsea permafrost is either absent or discontinuous to sporadic.

The correlation between the patterns of *in situ* sediment temperatures and permafrost extent can be extrapolated to other areas of the Arctic shelf, especially ESAS (Fig. 7). The Arctic shelf zone with sediment temperatures ≤ -0.6°C is restricted to sea depths within 80–100 m (120 m in the northern Laptev shelf), which agrees with the potential distribution of continuous subsea permafrost. The bottom sediment temperatures on the continental slope (>200 m sea depths) vary from −0.6 °C to +0.9°C and are mainly controlled by the warming effect of the Atlantic intermediate water mass traceable along the whole continental slope of Eurasia and North America. The anomalously low *in situ* sediment temperatures (about −1.5 °C) observed in some continental slope areas at sea depths 200–350 m, including the areas of methane seepage in the Laptev Sea, may be due to cold dense water cascading from the shelf or to dissociation of gas hydrates (Chuvilin et al., 2022). The latter hypothesis is supported by the P-T conditions of the sediments corresponding to the methane hydrate stability. The data collected in the cruises of 2019–2022 (Chuvilin et al., 2021a, 2022), as well as the data of drilling campaigns in 2011–2014 (Shakhova et al., 2017; Chuvilin et al., 2013), together with published evidence (Romanovskii and Hubberten, 2001; Romanovskii et al., 2004, 2005; Romanovskii and Tumskoy, 2011; Matveeva et al., 2020; Bogoyavlensky et al., 2022; Gavrilov et al., 2020a, 2020b), were used to compile a simplified map of permafrost distribution in the Russian Arctic seas (Fig. 8).

It shows that ice-bearing permafrost occurs on the Arctic shelf from the shoreline to the sea depths 80–100 m which correspond to offshore distances of ~800–1000 km in some areas. Permafrost is absent deeper offshore in shelf and continental slope areas tough may exist locally at sea depths within 120 m in the northern Laptev shelf (Chuvilin et al., 2022). In general, 100–600 m thick continuous subsea permafrost occurs at relatively large subbottom depths over a greater part of the Arctic shelf, especially in its eastern segment, beneath unfrozen (cryotic) saline shallow sediments. The subsea permafrost is sporadic and discontinuous along the northern limit of its extent at sea depths ~60 m and shallower, as well as in areas of high heat flux associated with basement faults (Krylov et al., 2020). Discontinuous and sporadic relic permafrost may also exist in the offshore areas exposed to the warming effect of the great Siberian rivers (Ob, Yenisei, and Lena).

There was a hypothesis that discontinuous relic marine permafrost might occupy ~120,000 km^2, including a greater part of the Laptev and East Siberian shelf, in the influence zone of the Lena River plume traceable as far as 700–800 km away from the delta. On the other hand, prominent water stratification and negative or subzero bottom water temperatures persisting all year round in the Laptev shelf north of the Lena delta (Semiletov et al., 2000) indicate conditions sufficient for maintaining continuous permafrost, except for areas of thermokarst paleolakes that existed prior to the latest transgression (Shakhova et al.,

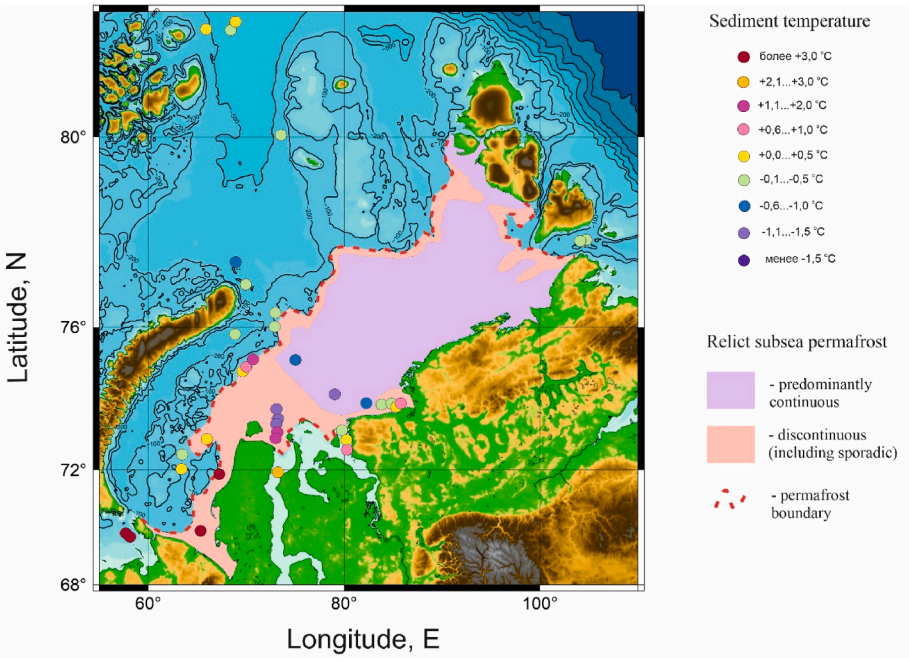

Fig. 6. Sediment temperatures and subsea permafrost in the Kara Sea.

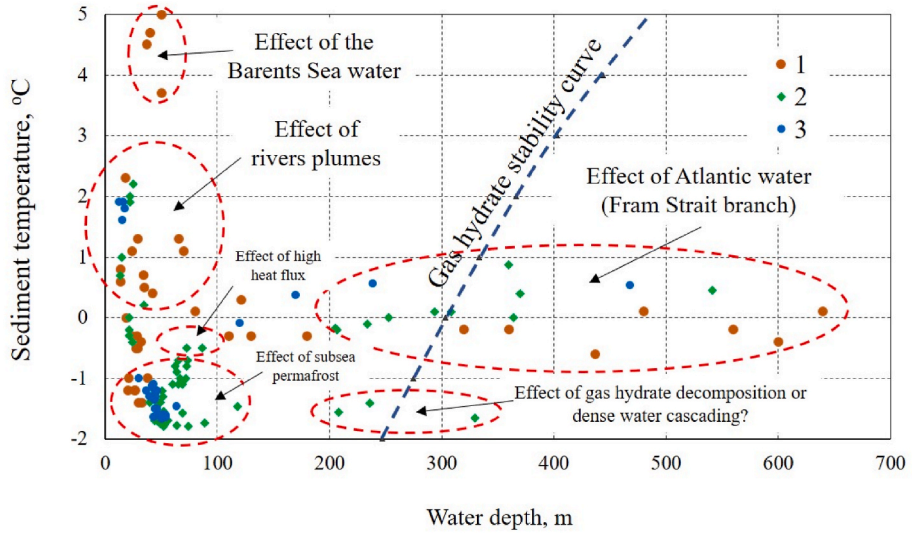

Fig. 7. Sediment temperatures vs. water depths for the Arctic seas. Symbols mark data from Kara (1), Laptev (2), and East Siberian (3) Arctic seas. Gas hydrate stability curve is as in Fig. 3.

2010b), and areas of high seismic, tectonic, and geothermal activity (Shakhova et al., 2019; Chuvilin et al., 2022). The warming effect of the Lena River was shown (Semiletov et al., 2005; Shakhova and Semiletov, 2007) to be of key importance in shallow shelf zones east and southeast of the Lena delta because of increasing wind-driven water mixing till the sea bottom. The increasing riverine inputs of the Lena warm up the bottom and surface sediments in summer to +2–3 °C in the vicinity of the Dmitry Laptev Strait and in the shallow southwestern part of the adjacent East Siberian Sea. However, the drilling and modeling data show that in general this warming effect is limited by deepening of the continuous subsea permafrost table and in some areas correlated with existence of seepage areas (Nicolsky and Shakhova, 2010; Fartyshev, 1993). However, existence of numerous seepage areas indicates on existence of gas pathways/through taliks, for example the Buor Khaya Gulf, where the Lena discharge has caused summer water warming up to +1°C in in the first decade of the 20th century (Shakhova et al., 2014). We consider formation of through taliks in such areas as a consequence of top-down integrative warming induced by the geological scale water-sediment thermal equilibration and recent enhanced river heating effect. In addition, several seepage areas were found in both seismo-tectonic active zones such as the Laptev Sea Rift, as well in the East Siberian Sea (Fig. 8), which is still considered as the passive continental margin and needs special marine studies.

5. Conclusions

The reported data confirm that the bottom sediment temperatures in the Arctic seas are distributed unevenly, especially in the Kara Sea shelf (from +5.0 °C in the west to −1.4 °C in the east). The high sediment temperatures in the western and central parts of the Kara Sea are due to the effect of warm water inputs: Atlantic currents coming from the Barents Sea through the Kara Gates strait; relatively warm fresh water from the large Siberian rivers (Ob, Yenisei, Pyasina, and Lena); Fram and Barents Sea branches of the Atlantic water currents in the northern and northwestern parts of the area. The distribution of bottom sediment temperatures correlates well with the presumed complex pattern of relic subsea permafrost, as it was shown for the case of the Kara Sea. In this respect, the bottom sediment temperature features in the Arctic seas can be used as a proxy of subsea permafrost distribution at relatively large subbottom depths.

The available field data and geological reports show that ice-bearing permafrost in the Siberian Arctic shelf extends from the shoreline till sea depths of 80–100 m, within the respective offshore distances of ~800–1000 km in some areas. Deeper offshore shelf and continental

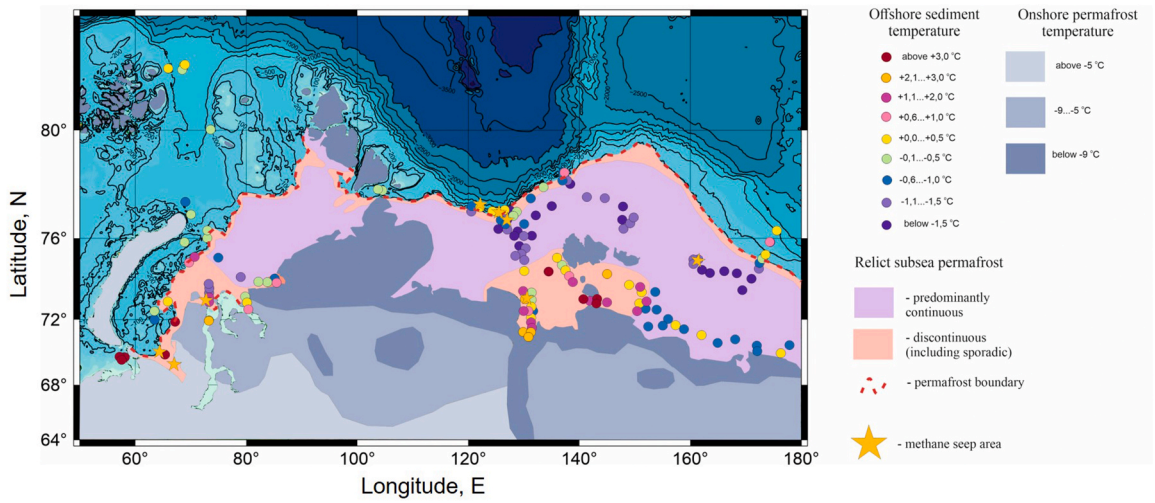

Fig. 8. Permafrost and temperature distribution in the Russian Arctic.

slope areas are free from permafrost, though its remnants may exist locally at sea depths within 120 m. In general, 100–600 m thick continuous subsea permafrost may occur in the Kara, Laptev, and East Siberian shelves, where the saline shallow sediments are unfrozen (cryotic). The subsea permafrost is sporadic and discontinuous along the northern limit of its extent at sea depths >70 m, as well as in zones of high heat flux associated with basement faults and in areas exposed to the warming effect of the Ob', Yenisei, and Lena riverine inputs. Future degradation of subsea permafrost may potentially lead to an increase methane releasing that has been long stored in permafrost environmental (in free gas or gas hydrate forms) and formation of new methane seep areas. Such seepage areas will be caused by top-down and/or upward heat fluxes associated spatially with submerged lake (or rivers) taliks and geothermal anomalies in the rift zones, correspondingly.

Additionally, 85% of all bottom sediments over the vast area of the Kara, Laptev, and East Siberian shelves were found out to consist of water-saturated silty clay and silt with rather uniform particle size distribution. The new thermal conductivity and heat capacity estimates for the Kara Sea agree with the values of 1.0 W/(m·K) and 2900 kJ/m^3, respectively, obtained previously from other Arctic seas. Another important result is that thermal conductivity becomes up to 40% higher depthward from 0 to 2 m subbottom depth, possibly, because of lower moisture content and porosity in lithified sediments.

Declaration of competing interest

The authors declare that they have no known competing financial interests or personal relationships that could have appeared to influence the work reported in this paper.

Data availability

Data will be made available on request.

Acknowledgments

This field-based study was supported by the Russian Science Foundation (RSF) (grant: 21-77-30001). Laboratory work was supported by the RSF grants 21-77-10074, 22-17-00112 and 22-67-00025. The study of water currents was partly supported by RSF grant 23-17-00087. Additional support was from the Skolkovo Institute of Science and Technology, and the Ministry of Science and Higher Education of the Russian Federation (grant "Priority-2030", Tomsk State University). The design and manufacturing of the cutting-ring set for sediment sampling by «Fablab and Machine Shop» (Skoltech) are specially appreciated. The cruise of the R/V *Akademik Mstislav Keldysh* was funded by grant 021-2021-0010 from the Ministry of Science and Higher Education of the Russian Federation.

Appendix A. Supplementary data

Supplementary data to this article can be found online at https://doi.org/10.1016/j.marpetgeo.2023.106467.

References

Andreassen, K., Hubbard, A., Winsborrow, M., Patton, H., Vadakkepuliyambatta, S., Plaza-Faverola, A., Gudlaugsson, E., Serov, P., Deryabin, A., Mattingsdal, R., Mienert, J., Bunz, S., 2017. Massive blow-out craters formed by hydrate-controlled methane expulsion from the Arctic seafloor. Science 356, 948–953. https://doi.org/10.1126/science.aal4500.

Angelopoulos, M., Westermann, S., Overduin, P.P., Faguet, A., Olenchenko, V., Grosse, G., Grigoriev, M.N., 2019. Heat and salt flow in subsea permafrost modeled with CryoGRID2. J. Geophys. Res.: Earth Surf. 124, 920–937. https://doi.org/10.1029/2018JF004823.

Angelopoulos, M., Overduin, P.P., Miesner, F., Grigoriev, M.N., Vasiliev, A.A., 2020. Recent advances in the study of Arctic submarine permafrost. Permafr. Periglac. Processes Special Issue: Trans. Int. Permafr. Assoc. No. 3 31 (3), 442–453. https://doi.org/10.1002/ppp.2061.

ASTM D422–63, 2007. Standard Test Method for Particle-Size Analysis of Soils. Annual Book of ASTM Standards.

Baranov, B.V., Lobkovsky, L.I., Dozorova, K.A., Tsukanov, N.V., 2019. The fault system controlling methane seeps on the shelf of the Laptev Sea. Dokl. Earth Sci. 486 (1), 571–574.

Bogoyavlensky, V., Kishankov, A., Yanchevskaya, A., Bogoyavlensky, I., 2018. Forecast of gas hydrates distribution zones in the Arctic Ocean and adjacent shore Areas. Geosciences 8, 453. https://doi.org/10.3390/geosciences8120453.

Bogoyavlensky, V.I., Kazanin, A.G., Kishankov, A.V., Kazanin, G.A., 2021. Earth degassing in the Arctic: comprehensive analysis of factors of powerful gas emission in the Laptev Sea. Arctic: Ecol. Econ. 2, 178–194. https://doi.org/10.25283/2223-4594-2021-2-178-194 (in Russian).

Bogoyavlensky, V., Kishankov, A., Kazanin, A., Kazanin, G., 2022. Distribution of permafrost and gas hydrates in relation to intensive gas emission in the central part of the Laptev Sea (Russian Arctic). Mar. Petrol. Geol. 138, 105527 https://doi.org/10.1016/j.marpetgeo.2022.105527.

Bogoyavlensky, V., Kishankov, A., Kazanin, A., Kazanin, G., 2023. Evidence of large-scale absence of frozen ground and gas hydrates in the northern part of the East Siberian Arctic shelf (Laptev and East Siberian seas). Mar. Petrol. Geol. 148, 106050 https://doi.org/10.1016/j.marpetgeo.2022.106050.

Chernykh, D., Yusupov, V., Salomatin, A., Shakhova, N., Gershelis, E., Konstantinov, A., Grinko, A., Chuvilin, E., Dudarev, O., Koshurnikov, A., Semiletov, I., 2020. Sonar estimation of methane bubble flux from thawing subsea permafrost: a case study from the Laptev sea shelf. Geosciences 10, 411. https://doi.org/10.3390/geosciences10100411.

Cheverev, V.G., Vidyapin, I.Yu, Tumskoy, V.E., 2007. Composition and characteristics of the thermokarst lagoon deposits, Bykovsky peninsula. Kriosfera Zemli 11 (3), 44–50.

Chuvilin, E.M., Bukhanov, B.A., Tumskoy, V.E., Shakhova, N.E., Dudarev, O.V., Semiletov, I.P., 2013. Thermal conductivity of bottom sediments in the region of Buor-Khaya Bay (shelf of the Laptev Sea). Kriosfera Zemli 17 (2), 32–40.

Chuvilin, E., Davletshina, D., Ekimova, V., Bukhanov, B., Shakhova, N., Semiletov, I., 2019. Role of warming in destabilization of intrapermafrost gas hydrates in the Arctic Shelf: experimental modeling. Geosciences 9, 407. https://doi.org/10.3390/geosciences9100407.

Chuvilin, E., Bukhanov, B., Grebenkin, S., Tumskoy, V., Shakhova, N., Dudarev, O., Semiletov, I., Spasennykh, M., 2021a. Thermal properties of sediments in the East siberian arctic seas: a case study in the buor-khaya Bay. Mar. Petrol. Geol. 123, 104672 https://doi.org/10.1016/j.marpetgeo.2020.104672.

Chuvilin, E., Grebenkin, S., Zhmaev, M., 2021b. Gas permeability of sandy sediments: effects of phase changes in pore ice and gas hydrates. Energy Fuels 35 (9), 7874–7882. https://doi.org/10.1021/acs.energyfuels.1c00366.

Chuvilin, E., Bukhanov, B., Yurchenko, A., Davletshina, D., Shakhova, N., Spivak, E., Rusakov, V., Dudarev, O., Khaustova, N., Tikhonova, A., Gustafsson, O., Tesi, T., Martens, J., Jakobsson, M., Spasennykh, M., Semiletov, I., 2022. In-situ temperatures and thermal properties of the East Siberian Arctic shelf sediments: key input for understanding the dynamics of subsea permafrost. Mar. Petrol. Geol. 138, 105550 https://doi.org/10.1016/j.marpetgeo.2022.105550.

Cruise Report, 2016a. SWERUS-C3. Leg 1. SU-AB, Stockholm, 978-91-87355-20-2.

Cruise Report, 2016b. SWERUS-C3. Leg 2. SU-AB, Stockholm, 978-91-87355-21-9.

Dmitrenko, I.A., Kirillov, S.A., Serra, N., Koldunov, N.V., Ivanov, V.V., Schauer, U., Polyakov, I.V., Barber, D., Janout, M., Lien, V.S., Makhotin, M., Aksenov, Y., 2014. Heat loss from the Atlantic water layer in the northern Kara Sea: causes and consequences. Ocean Sci. 10, 719–730. https://doi.org/10.5194/os-10-719-2014.

Durner, W., Iden, S.C., von Unold, G., 2017. The integral suspension pressure method (ISP) for precise particle-size analysis by gravitational sedimentation. Water Resour. Res. 53, 33–48. https://doi.org/10.1002/2016WR019830.

Dziublo, A., Storozheva, A., 2021. Technologies for efficient development of hydrocarbon resources on the Arctic and sub-Arctic shelf of Russia. In: Proc. of IOP Conf. Series: Earth and Environmental Science, 678, 012001. https://doi.org/10.1088/1755-1315/678/1/012001.

Egorov, A.S., Prischepa, O.M., Nefedov, Y.V., Kontorovich, V.A., Vinokurov, I.Y., 2021. Deep structure, tectonics and petroleum potential of the Western Sector of the Russian Arctic. J. Mar. Sci. Eng. 9, 258. https://doi.org/10.3390/jmse9030258, 2021.

Fartyshev, A.I., 1993. Features of Offshore Permafrost in the Laptev Sea Shelf. Nauka, Novosibirsk (in Russian).

Frenzel, B., Pécsi, M., Velichko, A. (Eds.), 1992. Atlas of Paleoclimates and Paleoenvironments of the Northern Hemisphere: Late Pleistocene-Holocene. Gustav Fischer, Stuttgart, Germany, p. 153.

Gavrilov, A., Pavlov, V., Fridenberg, A., Boldyrev, M., Khilimonyuk, V., Pizhankova, E., Buldovich, S., Kosevich, N., Alyautdinov, A., Ogienko, M., Roslyakov, A., Cherbunina, M., Ospennikov, E., 2020a. The current state and 125 kyr history of permafrost in the Kara Sea Shelf: modeling constraints. Cryosphere 14, 1857–1873. https://doi.org/10.5194/tc-2019-112.

Gavrilov, A., Malakhova, V., Pizhankova, E., Popova, A., 2020b. Permafrost and gas hydrate stability zone of the glacial part of the East-Siberian shelf. Geosciences 10, 484. https://doi.org/10.3390/geosciences10120484.

Grigoriev, N.F., 1966. Permafrost in the Yakutian Coastal Zone. Nauka, Moscow (in Russian).

Grigoriev, M.N., Imaev, V.S., Imaev, L.P., Koz'min, B.M., Kunitskiy, V.V., Mikulenko, K. I., Skriabin, R.M., Timirshin, K.V., 1996. Geological, Seismic and Cryogenic Processes in the Arctic Region of West Yakutia. Yakutian Science Center, Yakutsk (in Russian).

Guidelines for Soil Description, fourth ed., 2006. FAO, Rome, p. 97.

Gulas, S., Downton, M., D'Souza, K., Hayden, K., Walker, T.R., 2017. Declining Arctic Ocean oil and gas developments: opportunities to improve governance and

environmental pollution control. Mar. Pol. 75, 53–61. https://doi.org/10.1016/j.marpol.2016.10.014.
Günther, F., Overduin, P.P., Makarov, A.S., Grigoriev, M.N. (Eds.), 2013. Russian-German Cooperation System Laptev Sea: the Expeditions Laptev Sea – Mamontov Klyk 2011 & Buor Khaya 2012, 2013. Reports on Polar and Marine Research, vol. 113. Alfred Wegener Institute for Polar and Marine Research, Bremerhaven. https://doi.org/10.2312/BzPM_0664_2013, 664.
Hermann, R.R., Lin, N., Lebel, J., Kovalenko, A., 2022. Arctic transshipment hub planning along the Northern Sea Route: a systematic literature review and policy implications of Arctic port infrastructure. Mar. Pol. 145, 105275 https://doi.org/10.1016/j.marpol.2022.105275.
Kontorovich, A.E., Epov, M.I., Burshtein, L.M., Kaminskii, V.D., Kurchikov, A.R., Malyshev, N.A., Prischepa, O.M., Safronov, A.F., Stupakova, A.V., Suprunenko, O.I., 2010. Geology and hydrocarbon resources of the continental shelf in Russian Arctic seas and the prospects of their development. Russ. Geol. Geophys. 51 (1), 3–11. https://doi.org/10.1016/j.rgg.2009.12.003.
Koshurnikov, A.V., 2023. Permafrost of the Russian Arctic Seas Shelf (According to Geophysical Studies). Dc.Sc. Thesis. MSU, Moscow (in Russian).
Koshurnikov, A.V., Tumskoy, V.E., Shakhova, N.E., Sergienko, V.I., Dudarev, O.V., Gunar, A.Yu, Pushkarev, P.Yu, Semiletov, I.P., Koshurnikov, A.A., 2016. The first ever application of electromagnetic soundings for mapping of submarine permafrost table on the Laptev Sea shelf. Dokl. Earth Sci. 469, 860–863. https://doi.org/10.1134/S1028334X16080110.
Kozlov, S.A., 2006. Fundamentals of engineering and environmental studies of offshore oil and gas province in the Western Arctic. Neft' Gaz. 1, 1–5 (in Russian).
Krylov, A.A., Ivashchenko, A.I., Kovachev, S.A., Tsukanov, N.V., Kulikov, M.E., Medvedev, I.P., Ilinskiy, D.A., Shakhova, N.E., 2020. The seismotectonics and seismicity of the Laptev Sea region: the current situation and a first experience in a year-long installation of ocean bottom seismometers on the shelf. J. Volcanol. Seismol. 14, 379–393. https://doi.org/10.1134/S0742046320060044.
Lien, V.S., Trofimov, A.G., 2013. Formation of Barents Sea branch water in the northeastern Barents Sea. Polar Res. 32, 18905 https://doi.org/10.3402/polar.v32i0.18905.
Lobkovskiy, L., 2020. Seismogenic-triggering mechanism of gas emission activizations on the Arctic Shelf and associated phases of abrupt warming. Geosciences 11, 428. https://doi.org/10.3390/geosciences10110428.
Loktev, A.S., Bondarev, V.N., Kulikov, S.I., Rokos, S.I., 2012. Russian Arctic offshore permafrost. In: Offshore Site Investigation and Geotechnics, Proc. 7th Intern. Conf., London, pp. 579–586.
Loktev, A.S., Tokarev, M.Yu, Chuvilin, E.M., 2017. Problems and technologies of offshore permafrost investigation. Procedia Eng. 189, 459–465. https://doi.org/10.1016/j.proeng.2017.05.074.
Luchin, V.A., Semiletov, I.P., 2005. Interannual variability of water temperature in the Chukchi Sea. Dokl. Earth Sci. 405A (9), 1419–1422.
Luchin, V.A., Semiletov, I.P., Weller, G.E., 2002. Changes in the Bering Sea region: atmosphere–ice-water system in the second half of the twentieth century. Prog. Oceanogr. 55 (1–2), 23–44. https://doi.org/10.1016/S0079-6611(02)00068-X.
Makarov, D., Makarova, O., Mayurov, N., Mayurov, P., Turova, V., 2022. Development prospects and importance of the Northern Sea Route. Transport. Res. Procedia 63, 1114–1120.
Malakhov, V.V., Rimskaya-Korsakova, N.N., Osadchiev, A.A., Semiletov, I.P., Karaseva, N.P., Gantsevich, M.M., 2023. Findings of Pogonophores (Annelida and Siboglinidae) in the Kara Sea associated with the regions of dissociation of seafloor and cryogenic gas hydrates. Russ. J. Mar. Biol. 49 (2), 69–74. https://doi.org/10.1134/S1063074023020050.
Martens, J., Romankevich, E., Semiletov, I., Wild, B., Van Dongen, B., Vonk, J., Tesi, T., Shakhova, N., Dudarev, O.V., Kosmach, D., Vetrov, A., Lobkovsky, L., Belyaev, N., Macdonald, R.W., Pienkowski, A.J., Eglinton, T.I., Haghipour, N., Dahle, S., Carroll, M.L., Astrom, E.K.L., Grebmeier, J.M., Cooper, L.W., Possnert, G., Gustafsson, O., 2021. CASCADE-the circum-arctic sediment CArbon DatabasE. Earth Syst. Sci. Data 13, 2561–2572. https://doi.org/10.5194/essd-13-2561-2021.
Matveeva, T.V., Kaminsky, V.D., Semenova, A.A., Shchur, N.A., 2020. Factors affecting the formation and evolution of permafrost and stability zone of gas hydrates: case study of the Laptev Sea. Geoscience 12, 504. https://doi.org/10.3390/geosciences10120504.
Melnikov, V.P., Spesivtsev, V.I., 1995. Engineering-geological and Geocryological Conditions of the Shelf of the Barents and Kara Seas. Nauka, Novosibirsk (in Russian).
Nicolsky, D.J., Shakhova, N.E., 2010. Modelling sub-sea permafrost in the East-siberian arctic shelf: the Dmitry Laptev Strait. Environ. Res. Lett. 5 https://doi.org/10.1088/1748-9326/5/1/015006.
Nicolsky, D.J., Romanovsky, V.E., Romanovskii, N.N., Kholodov, A.L., Shakhova, N.E., Semiletov, I.P., 2012. Modelling sub-sea permafrost in the East siberian arctic shelf: the Laptev Sea region. J. Geophys. Res. 117, 429–436. https://doi.org/10.1029/2012JF002358.
Osadchiev, A.A., Frey, D.I., Shchuka, S.A., Tilinina, N.D., Morozov, E.G., Zavialov, P.O., 2021a. Structure of the freshened surface layer in the Kara Sea during ice-free periods. J. Geophys. Res.: Oceans 126, e2020JC016486. https://doi.org/10.1029/2020JC016486.
Osadchiev, A.A., Frey, D.I., Spivak, E.A., Shchuka, S.A., Tilinina, N.D., Semiletov, I.P., 2021b. Structure and inter-annual variability of the freshened surface layer in the Laptev and East-Siberian seas during ice-free periods. Front. Mar. Sci. 8, 735011 https://doi.org/10.3389/fmars.2021.735011.
Osadchiev, A., Viting, K., Frey, D., Demeshko, D., Dzhamalova, A., Nurlibaeva, A., Gordey, A., Krechik, V., Spivak, E., Semiletov, I., Stepanova, N., 2022. Structure and circulation of atlantic water masses in the St. Anna trough in the Kara Sea. Front. Mar. Sci. 9, 915674 https://doi.org/10.3389/fmars.2022.915674.
Overduin, P.P., Haberland, C., Ryberg, T., Kneier, F., Jacobi, T., Grigoriev, M.N., Ohrnberger, M., 2015. Submarine permafrost depth from ambient seismic noise. Geophys. Res. Lett. 42, 7581–7588. https://doi.org/10.1002/2015GL065409.
Overduin, P.P., Wetterich, S., Günther, F., Grigoriev, M.N., Grosse, G., Schirrmeister, L., Hubberten, H.-W., Makarov, A., 2016. Coastal dynamics and submarine permafrost in shallow water of the central Laptev Sea, East Siberia. Cryosphere 10, 1449–1462. https://doi.org/10.5194/tc-10-1449-2016.
Overduin, P.P., Schneider von Deimling, T., Miesner, F., Grigoriev, M.N., Ruppel, C., Vasiliev, A., Lantuit, H., Juhls, B., Westermann, S., 2019. Submarine permafrost map in the Arctic modeled using 1-d transient heat flux (SuPerMAP). J. Geophys. Res.: Oceans 124, 3490–3507. https://doi.org/10.1029/2018JC014675.
Pachauri, R.K., Meyer, L.A. (Eds.), 2014. Climate Change 2014: Synthesis Report. Contribution of Working Groups I, II and III to the Fifth Assessment Report of the Intergovernmental Panel on Climate Change. IPCC, Geneva, Switzerland, p. 151.
Portnov, A., Smith, A.J., Mienert, J., Cherkashov, G., Rekant, P., Semenov, P., Serov, P., Vanshtein, B., 2013. Offshore permafrost decay and massive seabed methane escape in water depths >20m at the South Kara Sea shelf. Geophys. Res. Lett. 40, 3962–3967. https://doi.org/10.1002/grl.50735.
Pribnow, D.F.C., Kinoshita, M., Stein, C.A., 2000. Thermal Data Collection and Heat Flow Recalculations for Ocean Drilling Program Legs 101-180. Institute for Joint Geoscientific Research, GGA, Hannover, Germany, 0120432. http://www-odp.tamu.edu/publications/heatflow/.
Rekant, P.V., Vasiliev, A.A., 2011. Distribution of subsea permafrost on the Kara Sea shelf. Earths Cryosphere 15 (4), 69–72.
Riedel, M., Wallmann, K., Berndt, C., Pape, T., Freudenthal, T., Bergenthal, M., Bunz, S, S., Bohrmann, G., 2018. In situ temperature measurements at the Svalbard Continental Margin: implications for gas hydrate dynamics. G-cubed 19, 1165–1177. https://doi.org/10.1002/2017GC007288.
Rokos, S.I., Dlugach, A.G., Loktev, A.S., Kostin, L.A., Kulikov, S.N., 2009. Permafrost of the Pechora and Kara seas shelf: genesis, composition, conditions of distribution and occurrence. Izhinernaya Geologiya 10, 38–41.
Romanovskii, N.N., Hubberten, H.-W., 2001. Results of permafrost modelling of the lowlands and shelf of the Laptev Sea region, Russia. Permafrost Periglacial Proc. 12, 191–202. https://doi.org/10.1002/ppp.387.
Romanovskii, N.N., Tumskoy, V.E., 2011. Retrospective approach to the estimation of the contemporary extension and structure of the shelf cryolithozone in East Arctic. Kriosfera Zemli 15 (1), 3–14.
Romanovskii, N.N., Kholodov, A.L., Gavrilov, A.V., Tumskoy, V.E., Hubberten, H.-W., Kassens, H., 1999. Ice-bonded permafrost thickness in the eastern part of the Laptev Sea shelf (results of computer simulation). Kriosfera Zemli 3 (2), 22–32.
Romanovskii, N.N., Gavrilov, A.V., Tumskoy, V.E., Kholodov, A.L., 2003. Cryolithozone of the East siberian arctic shelf. Moscow Univ. Geol. Bull. 4, 51–56 (in Russian).
Romanovskii, N.N., Hubberten, H.-W., Gavrilov, A.V., Tumskoy, V.E., Kholodov, A.L., 2004. Permafrost of the East siberian arctic shelf and coastal lowlands. Quat. Sci. Rev. 23, 1359–1369. https://doi.org/10.1016/j.quascirev.2003.12.014.
Romanovskii, N.N., Hubberten, H.-W., Gavrilov, A.V., Eliseeva, A.A., Tipenko, G.S., 2005. Offshore permafrost and gas hydrate stability zone on the shelf of East Siberian seas. Geo Mar. Lett. 25, 167–182. https://doi.org/10.1007/s00367-004-0198-6.
Rusakov, V.Y., Borisov, A.P., 2023. Sedimentation on the Siberian Arctic Shelf as an indicator of the arctic hydrological cycle. Anthropocene 41, 100370. https://doi.org/10.1016/j.ancene.2023.100370.
Sapart, C.J., Shakhova, N., Semiletov, I., Jansen, J., Szidat, S., Kosmach, D., Dudarev, O., van der Veen, C., Egger, M., Sergienko, V., Salyuk, A., Tumskoy, V., Tison, J.-L., Röckmann, T., 2017. The origin of methane in the East Siberian Arctic Shelf unravelled with triple isotope analysis. Biogeosciences 14, 2283–2292. https://doi.org/10.5194/bg-14-2283-2017.
Semenov, P., Portnov, A., Krylov, A., Egorov, A., Vanshtein, B., 2020. Geochemical evidence for seabed fluid flow linked to the subsea permafrost outer border in the South Kara Sea. Geochemistry 80, 125509. https://doi.org/10.1016/j.chemer.2019.04.005.
Semiletov, I.P., Savelieva, N.I., Weller, G.E., Pipko, I.I., Pugach, S.P., Gukov, A.Yu, Vasilevskaya, L.N., 2000. The dispersion of Siberian river flows into coastal waters: meteorological, hydrological, and hydrochemical aspects. In: Lewis, E.L. (Ed.), The Freshwater Budget of the Arctic Ocean, NATO Meeting/NATO ASI Series. Kluwer Academic Publishers, Dordtrecht, pp. 323–366.
Semiletov, I., Dudarev, O., Luchin, V., Shin, K.-H., Tanaka, N., 2005. The East-Siberian Sea as a transition zone between Pacific-derived waters and Artic shelf waters. Geophys. Res. Lett. 32 https://doi.org/10.1029/2005GL022490. L10614/2005GL022490.
Semiletov, I., Pipko, I., Gustafsson, Ö., Anderson, L.G., Sergienko, V., Pugach, S., Dudarev, O., Charkin, A., Gukov, A., Bröder, L., Andersson, A., Spivak, E., Shakhova, N., 2016. Acidification of East Siberian Arctic Shelf waters through addition of freshwater and terrestrial carbon. Nat. Geosci. 9, 361–365. https://doi.org/10.1038/ngeo2695.
Sergienko, V.I., Lobkovskii, L.I., Semiletov, I.P., Dudarev, O.V., Dmitrievskii, N.N., Shakhova, N.E., Romanovskii, N.N., Kosmach, D.A., Nikol'skii, D.N., Nikiforov, S.L., Salomatin, A.S., Anan'ev, R.A., Roslyakov, A.G., Salyuk, A.N., Karnaukh, V.V., Chernykh, D.B., Tumskoi, V.E., Yusupov, V.I., Kurilenko, A.V., Chuvilin, E.M., Bukhanov, B.A., 2012. The degradation of submarine permafrost and the destruction of hydrates on the shelf of East Arctic seas as a potential cause of the "methane catastrophe": some results of integrated studies in 2011. Dokl. Earth Sci. 446, 1132–1137. https://doi.org/10.1134/S1028334X12080144.

Serov, P., Portnov, A., Mienert, J., Semenov, P., Ilatovskaya, P., 2015. Methane release from pingo-like features across the South Kara Sea shelf, an area of thawing offshore permafrost. J. Geophys. Res., Earth Surf. 120, 1515–1529. https://doi.org/10.1002/2015JF003467.

Serov, P., Vadakkepuliyambatta, S., Mienert, J., Patton, H., Portnov, A., Silyakova, A., Panieri, G., Carroll, M.L., Carroll, J., Andreassen, K., Hubbard, A., 2017. Postglacial response of Arctic Ocean gas hydrates to climatic amelioration. Proc. Natl. Acad. Sci. U.S.A. 24, 6215–6220. https://doi.org/10.1073/pnas.1619288114.

Shakhova, N., Semiletov, I., 2007. Methane release and coastal environment in the East Siberian Arctic shelf. J. Mar. Syst. 66, 227–243. https://doi.org/10.1016/j.jmarsys.2006.06.006.

Shakhova, N.E., Semiletov, I.P., 2009. Methane hydrate feedbacks. In: Sommerkorn, M., Hassol, S.J. (Eds.), Arctic Climate Feedbacks: Global Implications. WWF International Arctic Programme, Ottawa, pp. 81–92, 978-2-88085-305-1.

Shakhova, N., Semiletov, I., Salyuk, A., Yusupov, V., Kosmach, D., Gustafsson, Ö., 2010a. Extensive methane venting to the atmosphere from sediments of the East siberian arctic shelf. Science 327, 1246–1250. https://doi.org/10.1126/science.1182221.

Shakhova, N., Semiletov, I., Leifer, I., Salyuk, A., Rekant, P., Kosmach, D., 2010b. Geochemical and geophysical evidence of methane release from the inner East Siberian Shelf. J. Geophys. Res. 115 https://doi.org/10.1029/2009JC005602.

Shakhova, N., Semiletov, I., Leifer, I., Sergienko, V., Salyuk, A., Kosmach, D., Chernykh, D., Stubbs, C., Nicolsky, D., Tumskoy, V., Gustafsson, Ö., 2014. Ebullition and storm-induced methane release from the East siberian arctic shelf. Nat. Geosci. 7 https://doi.org/10.1038/ngeo2007.

Shakhova, N., Semiletov, I., Sergienko, V., Lobkovsky, L., Yusupov, V., Salyuk, A., Salomatin, A., Chernykh, D., Kosmach, D., Panteleev, G., Nicolsky, D., Samarkin, V., Joye, S., Charkin, A., Dudarev, O., Meluzov, A., Gustafsson, Ö., 2015. The East Siberian Arctic Shelf: towards further assessment of permafrost-related methane fluxes and role of sea ice. Phil. Trans. Royal Soc. A 373, 20140451.

Shakhova, N., Semiletov, I., Gustafsson, O., Sergienko, V., Lobkovsky, L., Dudarev, O., Tumskoy, V., Grigoriev, M., Mazurov, A., Salyuk, A., Ananiev, R., Koshurnikov, A., Kosmach, D., Charkin, A., Dmitrevsky, N., Karnaukh, V., Gunar, A., Meluzov, A., Chernykh, D., 2017. Current rates and mechanisms of subsea permafrost degradation in the East Siberian Arctic Shelf. Nat. Commun. 8, 15872 https://doi.org/10.1038/ncomms15872.

Shakhova, N., Semiletov, I., Chuvilin, E., 2019. Understanding the permafrost–hydrate system and associated methane releases in the East Siberian Arctic Shelf. Geosciences 9, 251. https://doi.org/10.3390/geosciences9060251.

Shirokov, R.S., Vasiliev, A.A., 2019. Bathymetric and bottom temperatures GIS of the Barents and Kara seas. Nat. Res. Manag., GIS & Remote Sensing 1, 21–27.

Sloan, E.D., 1998. Clathrate Hydrates of Natural Gases, 2nd Ed.. Marcel Dekker, New York.

Soloviev, V.A., Ginzburg, G.D., Telepnev, E.V., Mikhaluk, Y.N., 1987. Cryothermia and Gas Hydrates in the Arctic Ocean. Sevmorgeologia, Leningrad, Russia (in Russian).

Steinbach, J., Holmstrand, H., Shcherbakova, K., Kosmach, D., Bruchert, V., Shakhova, N., Salyuk, A., Sapart, C.J., Chernykh, D., Noormets, R., Semiletov, I., Gustafsson, Ö., 2021. Source apportionment of methane escaping the subsea permafrost system in the outer Eurasian Arctic Shelf. In: Proceedings of National Academy of Sciences, the United States of America, vol. 10, e2019672118. https://doi.org/10.1073/pnas.2019672118.

Stranne, Ch, O'Regan, M., 2016. Conductive heat flow and nonlinear geothermal gradient in marine sediments – observation from Ocean Drilling Program boreholes. Geo Mar. Lett. 36, 25–33. https://doi.org/10.1007/s00367-015-0425-3.

Ulyantsev, A.S., Bratskaya, S.Yu, Polyakova, N.V., Trukhin, I.S., Parotkina, YuA., 2021. Dataset on pore water composition and grain size properties of bottom sediments and subsea permafrost from the Buor-Khaya Bay (Laptev Sea). Data Brief 39, 107580. https://doi.org/10.1016/j.dib.2021.107580.

Ulyantsev, A., Polyakova, N., Trukhin, I., Parotkina, Y., Dudarev, O., Semiletov, I., 2022. Peculiarities of pore water ionic composition in the bottom sediments and subsea permafrost: a case study in the Buor-Khaya Bay, 2022 Geosciences 12, 49, 10.3390/geosciences12020049 kriVasiliev.

Vasiliev, A.A., Streletskaya, I.D., Shirokov, R.S., Oblogov, G.E., 2011. Coastal permafrost evolution of western Yamal in context of climate change. Kriosfera Zemli 5 (1), 44–52.

Vasiliev, V.V., Viskunova, K.G., Kiyko, O.A., Kozlov, S.A., 2013. Geological map of the Russian federation. In: Scale 1: 1,000,000 (Third Generation). North of Kara and Barents Seas. VSEGEI, Saint-Petersburg (in Russian).

Winkler, M.M., 2018. Frontiers Arctic offshore exploration drilling business challenges. In: Proceedings of the Arctic Technology Conference. Huston, Texas, USA, 5–7 November 2018.

Yusupov, V., Salomatin, A., Shakhova, N., Chernykh, D., Domaniuk, A., Semiletov, I., 2022. Echo sounding for remote estimation of seabed temperatures on the Arctic Shelf. Geosciences 12, 315. https://doi.org/10.3390/geosciences12090315.

Zhang, X., Kong, G.-Q., Li, H., Wang, L., Yang, Q., 2022. Thermal conductivity of marine sediments influenced by porosity and temperature in the South China Sea. Ocean Eng. 260, 111992 https://doi.org/10.1016/j.oceaneng.2022.111992.